



# Reconstruction of east–west deep water exchange in the low latitude Atlantic Ocean over the past 25,000 years



Jacob N.W. Howe<sup>a,\*</sup>, Alexander M. Piotrowski<sup>a</sup>, Rong Hu<sup>a</sup>, Aloys Bory<sup>b</sup>

<sup>a</sup> Department of Earth Sciences, University of Cambridge, Downing Street, Cambridge, CB2 3EQ, UK

<sup>b</sup> Université de Lille, CNRS, Université du Littoral Côte d'Opale, UMR8187, LOG, Laboratoire d'Océanologie et de Géosciences, F-59000 Lille, France

## ARTICLE INFO

### Article history:

Received 19 February 2016

Received in revised form 18 October 2016

Accepted 24 October 2016

Available online 17 November 2016

Editor: M. Frank

### Keywords:

neodymium isotopes  
Last Glacial Maximum  
eastern Atlantic  
western Atlantic

## ABSTRACT

Radiogenic neodymium isotopes have been used as a water mass mixing proxy to investigate past changes in ocean circulation. Here we present a new depth transect of deglacial neodymium isotope records measured on uncleaned planktic foraminifera from five cores spanning from 3300 to 4900 m on the Mauritanian margin, in the tropical eastern Atlantic as well as an additional record from 4000 m on the Ceara Rise in the equatorial western Atlantic. Despite being located under the Saharan dust plume, the eastern Atlantic records differ from the composition of detrital inputs through time and exhibit similar values to the western Atlantic foraminiferal Nd across the deglaciation. Therefore we interpret the foraminiferal values as recording deep water Nd isotope changes. All six cores shift to less radiogenic values across the deglaciation, indicating that they were bathed by a lower proportion of North Atlantic Deep Water during the Last Glacial Maximum (LGM) relative to the Holocene. The eastern Atlantic records also show that a neodymium isotope gradient was present during the LGM and during the deglaciation, with more radiogenic values observed at the deepest sites. A homogeneous water mass observed below 3750 m in the deepest eastern Atlantic during the LGM is attributed to the mixing of deep water by rough topography as it passes from the western Atlantic through the fracture zones in the Mid-Atlantic Ridge. This implies that during the LGM the low latitude deep eastern Atlantic was ventilated from the western Atlantic via advection through fracture zones in the same manner as occurs in the modern ocean. Comparison with carbon isotopes indicates there was more respired carbon in the deep eastern than deep western Atlantic during the LGM, as is also seen in the modern Atlantic Ocean.

© 2016 The Authors. Published by Elsevier B.V. This is an open access article under the CC BY license (<http://creativecommons.org/licenses/by/4.0/>).

## 1. Introduction

Due to the important role that Atlantic meridional overturning circulation plays in regulating the Earth's climate, there is considerable interest in deciphering the proportion of northern- versus southern-sourced water masses occupying the deep Atlantic Ocean under different climatic regimes (Curry and Oppo, 2005; Sarnthein et al., 1994). The isotopes of the radiogenic element neodymium are increasingly being used to reconstruct changes in water mass mixing in the Atlantic Ocean in the recent geological past (e.g. Böhm et al., 2015; Gutjahr et al., 2008; Lippold et al., 2016; Piotrowski et al., 2004; Roberts et al., 2010; Skinner et al., 2013; Wei et al., 2016, amongst many others). To date, much of this work has focused upon changes in the north–south gradient in water mass mixing during the past ~25,000 years, including two re-

cent studies that revealed the distribution of neodymium isotopes predominantly in the western Atlantic during the Last Glacial Maximum (LGM) (Howe et al., 2016; Lippold et al., 2016).

At present there is a distinct lack of authigenic neodymium isotope records from the low latitude deep eastern Atlantic. Nutrient proxy reconstructions of the eastern Atlantic during the LGM all show lower benthic foraminiferal  $\delta^{13}\text{C}$  and/or higher Cd/Ca values than during the Holocene (Beveridge et al., 1995; Curry and Lohmann, 1983; Sarnthein et al., 1994). However, a comparison of neodymium isotope values to benthic foraminiferal  $\delta^{13}\text{C}$  revealed that  $\delta^{13}\text{C}$  was decoupled from water mass mixing in the deep western Atlantic during the LGM (Howe et al., 2016). Furthermore, the east–west offset in nutrient concentration in the modern Atlantic makes it difficult to determine whether the higher glacial nutrient concentrations in the eastern Atlantic were due to changes in water mass sourcing or respired organic matter content (Curry and Lohmann, 1990, 1983). The higher nutrient concentration in the modern eastern Atlantic than western Atlantic is in part due to a longer residence of deep waters in the east-

\* Corresponding author.

E-mail address: [jacob.howe@cantab.net](mailto:jacob.howe@cantab.net) (J.N.W. Howe).

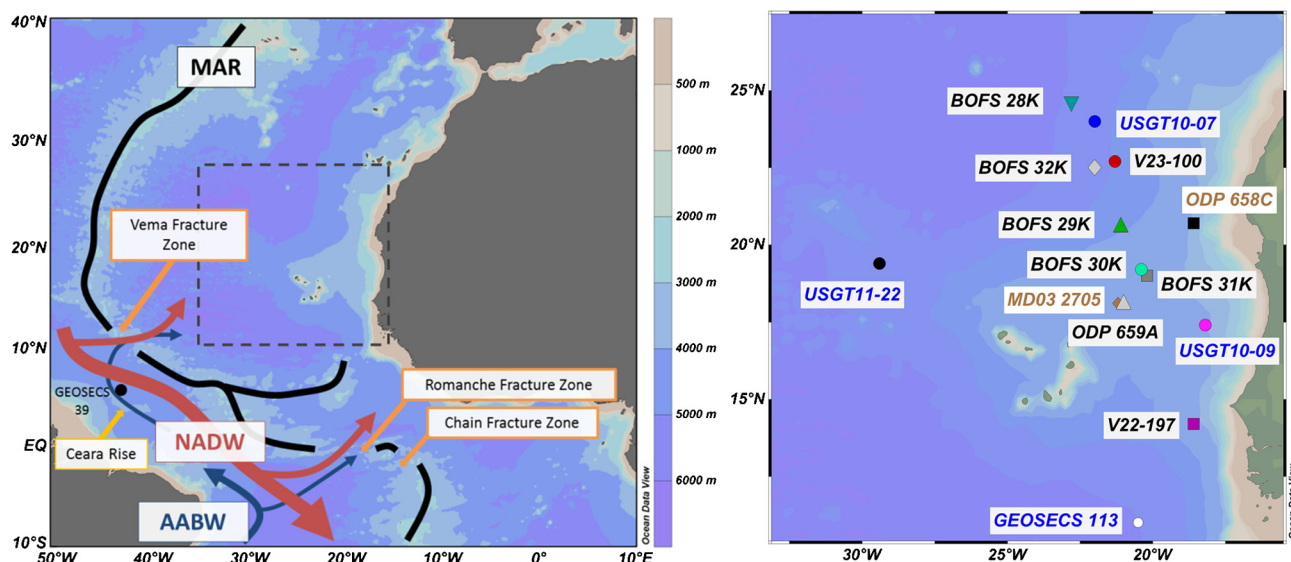


**Fig. 1.** Left: Map showing bathymetry and schematic of present-day deep water circulation in the low latitude Atlantic. Water masses labelled are North Atlantic Deep Water (NADW) and Antarctic Bottom Water (AABW). The Mid-Atlantic Ridge (MAR) is shown in black as separating the western and eastern basins below 3750 m, with the three major channels through which deep water is exchanged between these basins at low latitudes highlighted in orange. Dashed grey box marks the location of the inset map to the right. Also labelled are the Ceara Rise (location of ODP 928B and GeoB1515-1) and GEOSECS Station 39. Right: Regional map showing location of cores used to measure foraminiferal neodymium isotopes in this study BOFS 28K–32K, ODP 659A, V23-100 and V22-197 (locations listed in Table 1). Also shown are the location of seawater profiles USGT10-07, USGT10-09 and USGT11-22 (Stichel et al., 2015), GEOSECS Station 113 and core sites ODP 658C (Cole et al., 2009) and MD03 2705 (Jullien et al., 2007). (For interpretation of the references to colour in this figure legend, the reader is referred to the web version of this article.)

ern Atlantic (Broecker et al., 1980), but also due to higher surface productivity in the upwelling regions off the coast of Africa in the low latitude eastern Atlantic (Curry and Lohmann, 1990; Fariduddin and Loubere, 1997).

More recent studies have utilised the radiocarbon-based ages of bottom waters to infer changes in deep water ventilation rates in the eastern Atlantic over the deglaciation (e.g. Skinner et al., 2014), but the need to distinguish the radioactive decay of radiocarbon from changes in water mass mixing makes it difficult to use these results to determine water mass proportions. Meanwhile flow speed proxy reconstructions based on  $^{231}\text{Pa}/^{230}\text{Th}$  in the eastern Atlantic show distinct changes across the deglaciation (Gherardi et al., 2005) but do not provide information as to the origin of water masses ventilating the eastern Atlantic at those times. Whilst these proxies provide vital clues as to the dynamics of deep water circulation in the eastern Atlantic in the past, the lack of authigenic neodymium isotope data from the low latitude eastern Atlantic means that any potential changes in the exchange of deep water between the western and eastern basins of the low latitude Atlantic over the past 25 kyr are poorly constrained. In this study we present records of authigenic neodymium isotopes from five sites in the deep low latitude eastern Atlantic Ocean as well as one site in the deep equatorial western Atlantic for comparison. This east–west comparison along with consideration of nearby detrital neodymium isotope data leads us to conclude that these records are dominated by changes in water mass mixing in the past. We find that the deep low latitude eastern Atlantic was likely ventilated by waters from the western Atlantic in a similar manner during the LGM as it is today; however, with a greater proportion of southern-sourced waters.

### 1.1. Circulation in the low latitude deep Atlantic

In the modern western Atlantic Ocean, Antarctic Bottom Water extends as far north as the equator; whereas, in the deep eastern Atlantic its northward progress is impeded at around 30°S by the Walvis Ridge (Broecker et al., 1980). The low-latitude eastern Atlantic below the sill depth of the Mid-Atlantic Ridge,

**Table 1**

Locations of core sites in the Atlantic Ocean for which new uncleaned foraminiferal  $\varepsilon_{\text{Nd}}$  data is presented in this study.

	Latitude (°N)	Longitude (°E)	Depth (m)
<i>Deglacial records:</i>			
BOFS 28K	24.6	−22.8	4900
BOFS 32K	22.5	−22.0	4560
BOFS 29K	20.6	−21.1	4000
BOFS 30K	19.0	−20.2	3580
BOFS 31K	19.0	−20.2	3300
ODP 928B	6.0	−43.7	4010
<i>Time slice points:</i>			
V23-100	22.7	−21.3	4580
ODP 659A	18.1	−21.0	3070
V22-197	14.2	−18.6	3170

~3750 m, (Metcalf et al., 1964) is instead ventilated by northern- and southern-sourced waters which have mixed together as they pass through fracture zones in the equatorial region of the Mid-Atlantic Ridge (Mercier and Morin, 1997). North of the Sierra Leone Rise (~5°N) the eastern Atlantic below 3750 m is primarily ventilated via the Vema Fracture Zone at ~11°N (Fig. 1) (McCartney et al., 1991). In contrast, south of the Sierra Leone Rise, the deepest eastern Atlantic is ventilated by waters which pass through the Romanche and Chain Fracture Zones (Fig. 1) (Mercier and Morin, 1997).

The modern flux of deep water through the Vema Fracture Zone into the low-latitude northeastern Atlantic has been estimated at 2.1–2.4 Sv (McCartney et al., 1991) of which up to 1.1 Sv has been attributed to AABW (Rhein et al., 1998), although it has been shown that none of the water in the abyssal eastern Atlantic corresponds to pure AABW (Fig. 2) (Mercier and Morin, 1997; Metcalf et al., 1964). This fracture-zone-based ventilation regime leads to the deep eastern Atlantic Ocean displaying a different latitudinal mixing gradient between northern- and southern-sourced water masses to the western Atlantic (Fig. 2). Additionally, although there is unimpeded water mass communication between the western and eastern Atlantic at depths shallower than 3750 m,

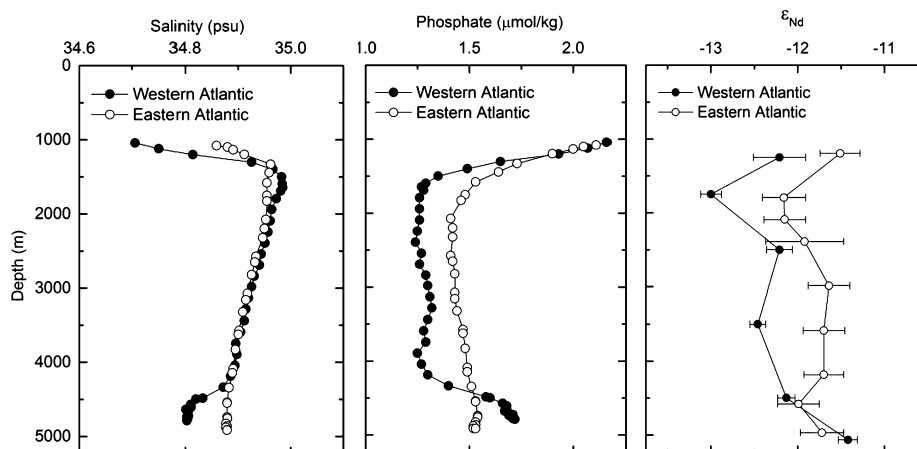


**Fig. 2.** Depth profiles below 1000 m of salinity and phosphate concentration in the modern low latitude Atlantic ocean from GEOSECS Station 39 in the western Atlantic (8.0°N, 43.9°W; filled circles) and GEOSECS Station 113 in the eastern Atlantic (11.0°N, 20.5°W; hollow circles), locations plotted in Fig. 1. Also shown in the depth profile of seawater  $\epsilon_{\text{Nd}}$  in the eastern (Station USGT11-22; 19.4°N, 29.4°W; Stichel et al., 2015) and western (Station 30.2; 18.6°N, 57.6°W; Lambelet et al., 2016) Atlantic.

seawater in the deep eastern Atlantic displays higher nutrient concentrations than at the corresponding depths in the western Atlantic (Fig. 2).

## 1.2. Nd isotopes

The neodymium isotopic composition ( $^{143}\text{Nd}/^{144}\text{Nd}$ ) of seawater is set by the weathering products of the continents (Goldstein and Hemming, 2003). It is expressed in epsilon notation as the deviation from the Chondritic Uniform Reservoir (CHUR)  $^{143}\text{Nd}/^{144}\text{Nd}$  ratio of 0.512638 (Jacobsen and Wasserburg, 1980) [ $\epsilon_{\text{Nd}} = ((^{143}\text{Nd}/^{144}\text{Nd}_{\text{sample}})/(^{143}\text{Nd}/^{144}\text{Nd}_{\text{CHUR}}) - 1) * 10^4$ ]. The unradiogenic (more negative)  $\epsilon_{\text{Nd}}$  values of seawater in the North Atlantic are set by the weathering products of circum-North Atlantic ancient cratons and their derived sediment (Goldstein and Hemming, 2003). This signal is exported to depth during deep water production leading to characteristic  $\epsilon_{\text{Nd}}$  values of  $-12.4$  to  $-13.2$  for North Atlantic Deep Water (NADW) (Lambelet et al., 2016) whereas southern-sourced Antarctic Bottom Water (AABW) that has more radiogenic values (around  $-8.5$ ) (Stichel et al., 2012). This has led to the neodymium isotopes being deemed a quasi-conservative tracer of water mass mixing (Frank, 2002).

The low latitude eastern Atlantic would be the ideal region to reconstruct the exchange of deep waters between the western and eastern basins of the Atlantic Ocean in the past. However, the low latitude eastern Atlantic represents a challenge for the use of neodymium isotopes as a tracer of past changes in water mass mixing. Although neodymium isotopes avoid the complication of biological dependence seen in the nutrient tracers, it has been shown the neodymium isotopic composition of sea water in the modern ocean can be modified by interaction with the continental margins by the process termed “boundary exchange” (Lacan and Jeandel, 2005). This includes certain regions of the modern low latitude eastern Atlantic where the neodymium composition of bottom water is modified by the benthic nepheloid layer (Stichel et al., 2015), which we take to be a manifestation of boundary exchange (Lacan and Jeandel, 2005). Furthermore, in this region the concentration of neodymium in seawater increases with depth (Stichel et al., 2015); an increasing neodymium concentration at depth is a universal phenomenon throughout the global ocean (Lacan et al., 2012) that is related to reversible scavenging (Siddall et al., 2008). As a particle-reactive element, Nd cannot behave as a truly conservative tracer, like salinity and temperature; however can be used as a quasi-conservative tracer (Frank, 2002) of water mass source in areas of strong lateral advection relative to reversible scavenging. Neodymium isotopes have been shown to trace water masses

with high fidelity in the northwestern Atlantic despite increasing neodymium concentrations with depth (Lambelet et al., 2016) indicating that sediment input and reversible scavenging do not preclude using Nd isotopes to trace the advection of water masses on long path-lengths in the deep ocean.

However, although the intermediate to deep eastern and western Atlantic exhibit similar salinity profiles (Fig. 2a), the eastern Atlantic clearly exhibits  $\epsilon_{\text{Nd}}$  values 0.5 to 1 epsilon units more radiogenic than corresponding depths in the western Atlantic (Fig. 2c). Taking into account the aforementioned evidence for reversible scavenging in the eastern Atlantic (Stichel et al., 2015), it seems likely that this offset likely reflects the reversible scavenging and export to depth of more radiogenic signature of intermediate depth Mediterranean Outflow Water signature in the eastern Atlantic relative to the unradiogenic Labrador Sea Water signature which is more prevalent in the northwest Atlantic (Jenkins et al., 2015; Lambelet et al., 2016). Finally, given that much of the low latitude eastern Atlantic sits under the Saharan dust plume (Grousset et al., 1998), the possibility that diagenetic reactions down-core may have overprinted the foraminiferal ferromanganese coatings with a dust-derived signal must also be kept in mind. The  $\epsilon_{\text{Nd}}$  of Saharan dust varies from  $-12.1$  to  $-17.9$ , although modern core top sediments in this region are largely within the range of  $-12.2$  to  $-14.8$  (Grousset et al., 1998). Although all of these factors represent challenges to the use of neodymium isotopes as a water mass tracer, the low latitude deep eastern Atlantic away from nepheloid layers appear to be the best candidate for reconstructing east–west water mass mixing gradients in the Atlantic across the past 25 kyr.

## 2. Material and methods

### 2.1. Sediment cores

Five sediment cores, BOFS 28K, BOFS 29K, BOFS 30K, BOFS 31K and BOFS 32K (Table 1), which span depths from 3300 to 4900 m on the northwest African margin off the coast of Mauritania (Fig. 1), were used in this work for constructing deglacial foraminiferal  $\epsilon_{\text{Nd}}$  records of the deep low latitude eastern Atlantic. These cores were collected on Cruise 53 of the R.R.S. Charles Darwin comprising Leg C of the 1990 Biogeochemical Ocean Flux Study (BOFS) Programme and sit under the Saharan Dust plume in the modern ocean (Grousset et al., 1998). BOFS 28K–31K have been used previously for nutrient-proxy-based paleoceanographic reconstructions in this region (Beveridge et al., 1995). Nearby cores V23-100 and ODP 659A were also used to make additional

**Table 2**  
Age control tie points for BOFS 28K–32K.

Core	Depth (cm)	ID	$^{14}\text{C}$ age	Age Sds	Species
BOFS 31K	0–1	SUERC-53704	3021	37	<i>Globigerinoides sacculifer</i>
BOFS 31K	19–20	SUERC-53706	8561	36	<i>G. sacculifer</i> / <i>Globigerinoides ruber</i>
BOFS 31K	26–27	SUERC-53707	9614	37	<i>G. sacculifer</i> / <i>G. ruber</i>
BOFS 31K	31–32	Planktic $\delta^{18}\text{O}$ minimum			
BOFS 31K	34–35	SUERC-53708	11,874	41	<i>G. sacculifer</i> / <i>G. ruber</i>
BOFS 31K	46–47	SUERC-53709	14,175	46	<i>G. sacculifer</i> / <i>G. ruber</i>
BOFS 31K	49–50	Planktic $\delta^{18}\text{O}$ minimum			
BOFS 31K	58–59	SUERC-53710	16,524	54	<i>G. sacculifer</i> / <i>G. ruber</i>
BOFS 30K	03–04	SUERC-53698	4292	35	<i>G. ruber</i>
BOFS 30K	21–22	SUERC-53699	8811	38	<i>G. ruber</i>
BOFS 30K	27–30	Turbidite			
BOFS 30K	37–38	Planktic $\delta^{18}\text{O}$ minimum			
BOFS 30K	41–42	SUERC-53700	12,585	42	<i>G. sacculifer</i> / <i>G. ruber</i>
BOFS 30K	44.5–49.5	Turbidite			
BOFS 30K	51–52	SUERC-53701	15,011	49	<i>G. ruber</i>
BOFS 30K	61–62	SUERC-54851	17,670	61	<i>G. sacculifer</i> / <i>G. ruber</i>
BOFS 29K	01–02	SUERC-53694	2928	37	<i>G. sacculifer</i>
BOFS 29K	15–16	SUERC-53695	6852	38	<i>G. sacculifer</i>
BOFS 29K	16.5–19.5	Turbidite			
BOFS 29K	27–28	Planktic $\delta^{18}\text{O}$ minimum			
BOFS 29K	35–36	SUERC-53696 (age reversal)	11,683	41	<i>G. sacculifer</i> / <i>G. ruber</i>
BOFS 29K	38–43	Turbidite			
BOFS 29K	47–48	Planktic $\delta^{18}\text{O}$ minimum			
BOFS 29K	51–52	SUERC-53697	18,671	63	<i>G. sacculifer</i> / <i>G. ruber</i>
BOFS 32K	0–1	SUERC-53714	3713	37	<i>G. sacculifer</i>
BOFS 32K	13–14	SUERC-53715	6851	36	<i>G. sacculifer</i>
BOFS 32K	42–47	Turbidite			
BOFS 32K	42–43	SUERC-53716 (age reversal)	24,157	110	<i>G. sacculifer</i> / <i>G. ruber</i>
BOFS 32K	55–56	SUERC-53717	23,056	98	<i>G. sacculifer</i>
BOFS 28K	0–1	32K core top age			
BOFS 28K	13.5–17.5	Turbidite			
BOFS 28K	22–23	Planktic $\delta^{18}\text{O}$ minimum			
BOFS 28K	25–26	Planktic $\delta^{18}\text{O}$ maximum			
BOFS 28K	29–30	Planktic $\delta^{18}\text{O}$ minimum			
BOFS 28K	30+	Turbidite			

Holocene and LGM measurements, whilst V22-197 was used to make just a Holocene measurement (Cores locations are plotted in Fig. 1 and listed in Table 1). All eight of these cores are bathed by Northeast Atlantic Deep Water today with little indication of the influence of Antarctic Bottom Water from nearby salinity measurements (Fig. 2). An additional deglacial foraminiferal  $\varepsilon_{\text{Nd}}$  record was also constructed for site ODP 928B on the Ceara Rise (Fig. 1; Table 1) in the deep western equatorial Atlantic in order to compare neodymium isotopes along the flow path of deep water communication between the western and eastern basins of the low latitude Atlantic Ocean.

## 2.2. Age models

The published age models of BOFS 29K–31K, based upon benthic foraminiferal  $\delta^{18}\text{O}$  (Beveridge et al., 1995), were recalibrated by measuring new radiocarbon dates at the Scottish Universities Environmental Research Centre (SUERC) Glasgow on, where possible, monospecific samples (>10 mg) of the planktic species *Globigerinoides sacculifer* or *Globigerinoides ruber* from BOFS 29K–32K (Table 2). BOFS 28K was not radiocarbon dated due to the low sedimentation rate and heavy bioturbation (Beveridge et al., 1995). Additional age constraints were obtained by tying planktic foraminiferal  $\delta^{18}\text{O}$  to the ice-core-tied age model of planktic foraminiferal  $\delta^{18}\text{O}$  from MD95-2042 (Shackleton et al., 2000). Radiocarbon ages were converted to calendar age using the MARINE13 calibration (Reimer et al., 2013), the assumption of constant reservoir age in this region is based upon a modelling study (Butzin et al., 2005). Turbidites were identified and their intervals were removed from the deglacial age models of BOFS 28K, 29K, 30K and 32K (Beveridge et al., 1995). The final age models were constructed in BChron using the combination of radiocarbon

dates and stable isotope tie points detailed in Table 2. The final sedimentation rates vary from 2 to 3 cm/kyr according to their proximity to the Saharan dust plume. The veracity of age models were checked by comparing the stable isotope records of each core against that of BOFS 31K (Fig. 3 and Fig. S1) as that core had no turbidite layers identified in the depth range of interest and has the highest resolution stable isotope records and most age control tie points. The greatest element of uncertainty in the age models of the other cores is the effect of the turbidite layers (grey bars; Figs. S1 and S2) that were assigned, via inspection of the cores, in previous work for BOFS 28K, 29K and 30K (Beveridge, 1995) and, from XRF data, in this work for BOFS 32K (Fig. S2). The radiocarbon dates (Table 2) along with the trends in planktic and benthic oxygen isotopes (Fig. 3) suggest that the turbidites did not cause major shifts in sedimentation rate. Indeed the samples from the sections classed as turbidites from BOFS 29K appear to show very similar trends as samples from nearby depths (Fig. S1), suggesting that these turbidites were minor disturbances in the sediment and the material deposited by the turbidites came from nearby depths. Although there is slight uncertainty in the age ranges spanned by these turbidites, the assumption that sedimentation continued linearly across them produces coherent age models for the benthic and planktic foraminiferal oxygen isotopes (Fig. 3c and 3d), whereas if the depth ranges including the turbidites were removed entirely from the age model as was originally done (Beveridge, 1995) then it introduces unreasonable steps in the stable isotope records. This was the justification for adopting the approach taken in this work of continuing the age models across the turbidites even though they are redeposited material.

Published age models based upon benthic foraminiferal  $\delta^{18}\text{O}$  were used to determine LGM depths in V23-100 (Sarnthein et al., 1994) and ODP 659A (Tiedemann et al., 1994). The published age



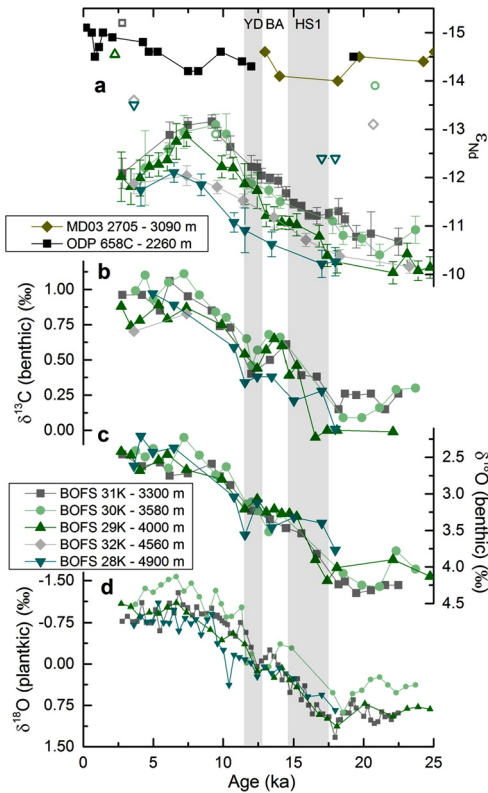


**Fig. 3.** (a) Deglacial  $\epsilon_{\text{Nd}}$  records for BOFS 28K–32K measured on uncleaned planktic foraminifera (filled symbols) contrasted with the detrital composition of the same cores (hollow symbols) (Bory, 1997; Grousset et al., 1998) and the nearby cores ODP 658C (20.7°N, 18.6°W, 2260 m, black squares) (Cole et al., 2009) and MD03 2705 (18.1°N, 21.2°W, 3090 m, gold diamonds) (Jullien et al., 2007). Error bars are the  $2\sigma$  analytical error of foraminiferal measurements. Deglacial benthic foraminiferal (b)  $\delta^{13}\text{C}$  and (c)  $\delta^{18}\text{O}$  records from BOFS 28K–32K measured on *Cibicidoides wuellerstorfi* (Beveridge et al., 1995) plotted on new radiocarbon based age models from this study. (d) Planktic foraminiferal  $\delta^{18}\text{O}$  of *Globigerinoides ruber* for BOFS 28K–31K (Beveridge, 1995) on the age models assigned in this work. Climate periods labelled are the Younger Dryas (YD), Bølling-Allerød (BA) and Heinrich Stadial 1 (HS1).

model of ODP 928B is based on planktic foraminiferal radiocarbon data (Howe et al., 2016).

### 2.3. Analytical procedures

Chemically uncleaned planktic foraminifera samples were prepared for neodymium isotopic analysis following the procedures of Roberts et al. (2010). Samples were measured on either a Nu Plasma or a NeptunePlus Multi Collector Inductively Coupled Plasma Mass Spectrometer at the University of Cambridge. Results were corrected for internal mass fractionation using an exponential mass correction to a  $^{146}\text{Nd}/^{144}\text{Nd}$  ratio of 0.7219. Samples were bracketed by concentration matched JNdi-1 standards which were corrected to the accepted value of 0.512115 (Tanaka et al., 2000). Reported errors are the  $2\sigma$  external error of the bracketing standards unless the internal error was greater, in which case the combined internal and external error is reported. The average external errors for samples run on the Nu and NeptunePlus were  $\pm 0.40$  and  $\pm 0.20$  epsilon units respectively.

## 3. Results

The core top planktic foraminiferal  $\epsilon_{\text{Nd}}$  values of BOFS 28K–32K, V23-100 and ODP659A all fall within the error bounds of both the nearest seawater profile and a seawater profile further away from the continental margin in the eastern Atlantic Ocean (Fig. 4). In contrast, the core top value of V22-197 from further south on

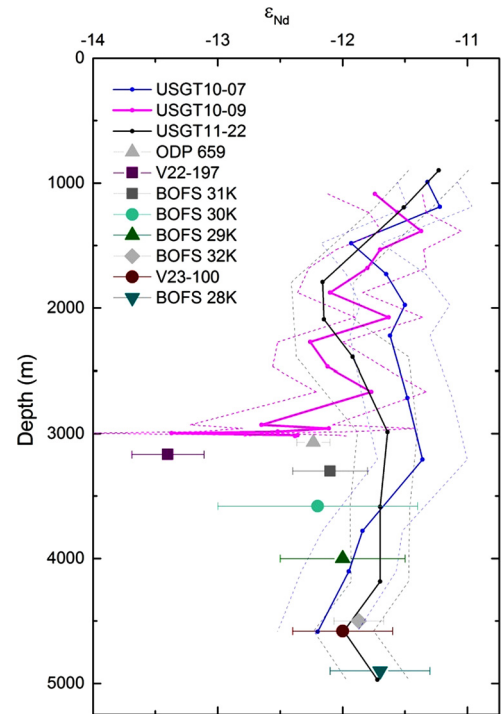


**Fig. 4.** Modern seawater  $\epsilon_{\text{Nd}}$  from nearby sites USGT10-07 (24.0°N, 22.0°W; blue line) USGT10-09 (17.4°N, 18.3°W; pink line) and open ocean site USGT11-22 (19.4°N, 29.4°W; black line) (Stichel et al., 2015) with  $\epsilon_{\text{Nd}}$  measurements made on uncleaned foraminifera from late Holocene samples of BOFS 28K–32K, V23-100, ODP659A and V22-197 with  $2\sigma$  error bars. All site locations are plotted in Fig. 1 and listed in Table 1; dashed lines indicate  $2\sigma$  error bounds of seawater  $\epsilon_{\text{Nd}}$  measurements. (For interpretation of the references to colour in this figure legend, the reader is referred to the web version of this article.)

the Mauritanian margin exhibits less radiogenic values than the other cores, more similar to seawater values measured at a nearby station that was identified to be influenced by a benthic nepheloid layer (Stichel et al., 2015). The five deglacial authigenic  $\epsilon_{\text{Nd}}$  records from BOFS 28K–32K (Fig. 3a) all shift from their most radiogenic values (−10 to −11) during the LGM to an unradiogenic peak (−12 to −13) in the early Holocene then converge at values around −12 in the late Holocene. The deglacial record of ODP 928B from the Ceara Rise in the western Atlantic is very similar to that of BOFS 29K from the same depth but slightly further north in the eastern Atlantic, except during the LGM when ODP 928B exhibits slightly more radiogenic values than BOFS 29K (Fig. 5). In the eastern Atlantic records there are neodymium isotopic gradients to more radiogenic values with increasing depth of 1 epsilon unit per 1500 m and 1.5 epsilon units per 1500 m during the LGM and the deglaciation respectively; this gradient collapses during the Holocene (Fig. 3a). Unlike the foraminiferal  $\epsilon_{\text{Nd}}$  records the detrital  $\epsilon_{\text{Nd}}$  values of nearby sites ODP 658C and MD03 2705 show little variability across the last 25 kyr and no early Holocene peak (Fig. 3a). The detrital  $\epsilon_{\text{Nd}}$  values from BOFS 28K–32K, available at much lower resolution, are in general more radiogenic than, but overall show similar trends to, the detrital records of ODP 658C and MD03 2705 (Fig. 3a).

## 4. Discussion

### 4.1. Core tops and modern seawater

The agreement of the core top  $\epsilon_{\text{Nd}}$  values from BOFS 28K–32K, V23-100 and ODP 659A with nearby seawater measurements (Fig. 4) provides confidence that planktic foraminifera at these sites are preserving the  $\epsilon_{\text{Nd}}$  of seawater in the deep low latitude

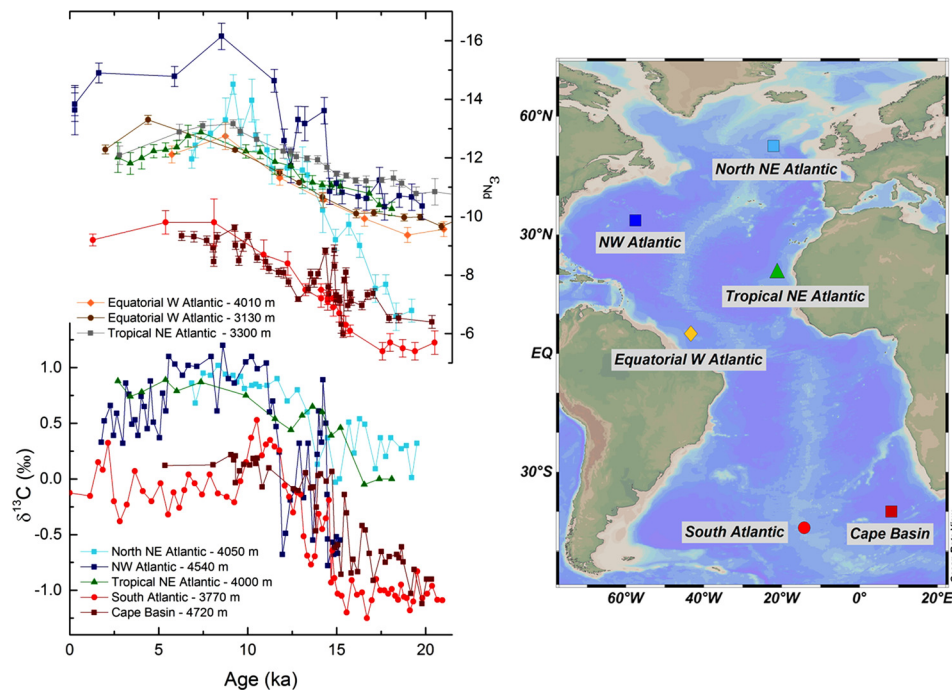


**Fig. 5.** **Top:** Deglacial records of authigenic  $\epsilon_{Nd}$  from deep sites throughout the Atlantic Ocean: the Rockall Basin in the northern northeast Atlantic (light blue squares; BOFS 8K, 52.5°N, 22.1°W, 4045 m) (Piotrowski et al., 2012), the Bermuda Rise in the northwest Atlantic (dark blue squares; OCE326-GGC6, 33.7°N, 57.6°W, 4541 m) (Roberts et al., 2010), the South Atlantic (burgundy squares; MD07-3076; 44.1°S, 14.2°W, 3770 m) (Skinner et al., 2013) and the Cape Basin (red squares; RC11 83; 41.1°S, 9.7°E, 4720 m) (Piotrowski et al., 2004) compared with GeoB1515-1 (brown; Lippold et al., 2016) and ODP 928B (orange) from the Ceara Rise in the equatorial Atlantic and BOFS 31K (grey) and BOFS 29K (green) from the Mauritanian margin in the tropical eastern Atlantic. **Bottom:** Deglacial carbon isotope records measured on benthic foraminiferal calcite (*Cibicides* species) from the same sites in the northern northeast Atlantic (Barker et al., 2004), the tropical eastern Atlantic (Beveridge et al., 1995), the South Atlantic (Waelbroeck et al., 2011) and the Cape Basin (Charles and Fairbanks, 1992) and from a sister site on the Bermuda Rise (ENO120 GGC1; 33.7°N, 57.6°W, 4450 m) (Boyle and Keigwin, 1987). **Right:** Map showing core locations. (For interpretation of the references to colour in this figure legend, the reader is referred to the web version of this article.)

eastern Atlantic. Furthermore, the agreement of the core top  $\epsilon_{Nd}$  values with the seawater profile from a site further away from the continental margin suggests that the Nd isotopic composition the foraminifera records can be considered a basin-wide record of Nd isotopes rather than local inputs (Rickli et al., 2009). This contrasts with the core top value of V22-197 that is less radiogenic than the other sites, but agrees well with another seawater profile that was identified to be influenced by a benthic nepheloid layer (Stichel et al., 2015). This demonstrates that planktic foraminifera preserve the boundary exchange signature of bottom water modified by the benthic nepheloid layer in such locations and highlights the importance of careful site selection to avoid such regions. Our core top data suggest that the core sites BOFS 28K–32K are suitable for reconstructing past water mass mixing changes in the deep low latitude eastern Atlantic, but cores such as V22-197, which are influenced more by boundary exchange, are not. We note that if there were a dissolved sedimentary boundary flux at the BOFS sites that had the same composition as seawater we would not be able to distinguish it in the core top values. However, we conclude that the difference in boundary exchange observed at these BOFS sites and V22-197 is more likely due to greater riverine sediment input from sub-Saharan rivers draining Gambia, Senegal and Guinea influencing the more southerly location of core V22-197, or because the latter core site is located under a region of high surface ocean productivity increasing the organic content of the benthic nepheloid layers (Fariduddin and Loubere, 1997).

#### 4.2. Down-core preservation of $\epsilon_{Nd}$ signal by foraminifera

The deglacial foraminiferal  $\epsilon_{Nd}$  record of ODP 928B is in good agreement with the published records from shallower depths on the Ceara Rise (Lippold et al., 2016), although the deeper record

exhibits slightly more radiogenic values indicating a greater proportion of more radiogenic southern-sourced waters (Fig. 5). The glacial values of the Ceara Rise cores fit well within the spatial pattern of neodymium isotopes in the western Atlantic during the LGM (Howe et al., 2016; Lippold et al., 2016) indicating that they represent advected seawater values. The coherency between the  $\epsilon_{Nd}$  records from the Ceara Rise and the Mauritanian margin (Fig. 5) then suggests that the eastern Atlantic records likely also reflect past changes in water mass mixing proportions, rather than local boundary exchange signals.

The lack of correlation between the foraminiferal  $\epsilon_{Nd}$  deglacial records of BOFS 28K–32K and the detrital values from the same cores and two nearby cores (Fig. 3) also suggests that the detrital component is not controlling the down-core foraminiferal  $\epsilon_{Nd}$  signal in the eastern Atlantic. If the  $\epsilon_{Nd}$  of Saharan dust ( $\epsilon_{Nd} = -12.1$  to  $-17.9$ ; Grousset et al., 1998) was affecting the Nd isotopic composition preserved in the coatings of the foraminifera down-core, the records would be expected to exhibit less radiogenic values, typical of seawater near benthic nepheloid layers in the modern eastern Atlantic (pink line, Fig. 4) (Stichel et al., 2015), during the LGM. Instead, the records all show more radiogenic values during the LGM (Fig. 3), indicating that the detrital composition cannot be invoked to explain the observed deglacial changes in the foraminiferal  $\epsilon_{Nd}$ . Furthermore, there is no indication of an unradiogenic early Holocene peak, as seen in the foraminiferal records, in the detrital  $\epsilon_{Nd}$  records (Fig. 3). Collectively these observations are evidence that the boundary exchange process that modifies bottom water neodymium near site V22-197 (Fig. 4) in the modern ocean, did not influence the BOFS cores during the last 25 kyr.

Despite the uncertainty in the age models, no realignment of the age models can completely remove the neodymium isotope gradient observed between our sites or alter the conclusions of

this work. Despite the low sedimentation rate of some of these cores, the neodymium isotope gradient observed in the past is not consistent with bioturbation muting the glacial–interglacial change at these sites. This is because if bioturbation were heavily “blurring” the signal in the sediment then the lower-sedimentation-rate deeper cores (BOFS 28K, 29K and 32K) should have their more extreme values and thus their glacial–interglacial change muted relative to the higher-sedimentation-rate shallower cores (BOFS 31K and 30K). Instead the deeper cores exhibit more extreme radiogenic values during the LGM and also have a larger LGM to core top shifts than the shallower sites (Fig. 3). Although the deeper and lower sedimentation rate cores BOFS 28K and 32K do show less radiogenic early Holocene values than the shallower higher sedimentation rate cores, it is important to note that BOFS 29K, which has a similar sedimentation rate to the deeper cores, exhibits an unradiogenic early Holocene peak in Nd isotopes, similar to the shallower higher sedimentation rate cores. This observation indicates that the difference between these cores cannot be an artefact of sedimentation rate. Furthermore a similar phenomenon of more radiogenic Holocene values at deeper sites is also seen in the Ceara Rise cores from the western Atlantic (Fig. 5), suggesting that it reflects a greater proportion of southern-sourced water at the deeper sites. Additionally, a glacial turbidite from BOFS 32K exhibits  $\epsilon_{\text{Nd}}$  values one epsilon unit less radiogenic than surrounding glacial values that come from 5 cm depth away within the core (Fig. S2). This result indicates that bioturbation is not “blurring out” signals spanning distances more than  $\sim 5$  cm, which is consistent with the typical reported depth of bioturbation (Teal et al., 2008). Additionally, the glacial values seen at the sites from the Mauritanian margin and Ceara Rise are similar to those observed at the deep Bermuda Rise (Fig. 5); that Bermuda Rise site has an extremely high accumulation rate thus cannot have lost its glacial signal due to bioturbation (Roberts et al., 2010). Finally, it is important to note that BOFS 28K, the deepest core with the lowest sedimentation rate does not show dampened glacial–interglacial changes in any of the stable isotope records relative to the other cores (Fig. 3). This reveals that the dampened early Holocene neodymium isotope peak cannot be due to bioturbation as the foraminiferal stable isotope records would, in that case, be similarly mixed and therefore muted. Although these observations do not rule out the effect of bioturbation over small distances within the these sediment cores, they indicate that bioturbation is not dominating the down core signal of all of these records and thereby demonstrate that neodymium isotope gradient must be reflective of a real difference in the water column in the past.

#### 4.3. Deglacial circulation changes in the deep tropical eastern Atlantic Ocean

The general trend of all sites to less radiogenic profiles across the glacial–interglacial transition (Figs. 3 and 5) is consistent with the resumption of strong NADW production during deglaciation and supports other proxy records (Boyle and Keigwin, 1987; Charles and Fairbanks, 1992; Gherardi et al., 2005; Piotrowski et al., 2004; Skinner et al., 2014). The neodymium isotope gradient between BOFS 28K–32K in the eastern Atlantic is observed during the LGM and throughout the deglaciation but collapses in the mid-Holocene (Fig. 3a). This gradient represents a significant change in water mass geometry because (1) the deepest site (BOFS 28K; 4900 m) and the shallowest site (BOFS 31K; 3300 m) are outside of analytical error of one another and (2) no realignment of the age models could make the peak values of those sites overlap within error as the unradiogenic early Holocene peak in BOFS 28K is one  $\epsilon_{\text{Nd}}$  unit more radiogenic than at BOFS 31K. The loss of the neodymium isotope gradient during the mid-Holocene – creat-

ing the modern water mass homogeneity observed at this location (Fig. 2) – indicates all of these sites being bathed by NADW.

The benthic foraminiferal  $\delta^{13}\text{C}$  records from BOFS 28K–32K support the notion of a depth-dependent water mixing gradient with lower values observed at the deeper sites (Fig. 3b) particularly during the LGM (Fig. 6). Interestingly, however, the  $\delta^{13}\text{C}$  records show a reversal in the Younger Dryas while the  $\epsilon_{\text{Nd}}$  records do not show any appreciable millennial scale variability across the deglaciation (Fig. 3). A radiocarbon reconstruction from the Iberian margin also shows better ventilated bottom waters during the Bølling–Allerød and more poorly ventilated bottom waters during the Younger Dryas (Skinner et al., 2014). A  $^{231}\text{Pa}/^{230}\text{Th}$  from the northeastern Atlantic also suggest slightly stronger circulation during the Bølling–Allerød (Gherardi et al., 2005). These  $\delta^{13}\text{C}$ , radiocarbon and  $^{231}\text{Pa}/^{230}\text{Th}$  shifts could theoretically represent changes in both the amount of respired organic matter and the deep water ventilation rate in the deep eastern Atlantic, without accompanying changes in deep water mass mixing proportions. However, deglacial  $\epsilon_{\text{Nd}}$  records from the Bermuda Rise (Böhm et al., 2015; Roberts et al., 2010) reveal that the deglacial trend of the neodymium isotopic composition of deep water becoming less radiogenic reversed during the Younger Dryas in the deep western Atlantic. The lack of  $\epsilon_{\text{Nd}}$  change at the Mauritanian margin would thus also have to represent different changes in the neodymium isotopic composition of the eastern and western Atlantic during the Younger Dryas. Alternatively, the transient  $\epsilon_{\text{Nd}}$  change in ocean circulation observed in the western Atlantic during the Younger Dryas may have been lost in these cores that have a low sedimentation rate (2 to 3 cm/kyr) in comparison to the high sedimentation rate Bermuda Rise site ( $\sim 20$  cm/kyr) (Roberts et al., 2010).

Bioturbation alone cannot explain the presence of a  $\delta^{13}\text{C}$  reversal but not an  $\epsilon_{\text{Nd}}$  reversal as it would be expected to affect both signals equally. Rather this discrepancy may reflect the processes by which these two signals are incorporated by foraminifera. The neodymium signal of bottom water is preserved by ferromanganese coatings formed on planktic foraminiferal tests whilst they are located in oxic bottom/pore waters near the sediment–water interface (Roberts et al., 2012, 2010). Given the low sedimentation rate they remained near the sediment–water interface for over one thousand years. Assuming the shallow pore waters reflect bottom water composition during this time, the planktic foraminifera will preserve a time-integrated bottom water signal thereby removing any transient change in Nd isotopes that may have been associated with the Younger Dryas and producing smoothed deglacial records (Fig. 3). In contrast, benthic foraminifera preserve the  $\delta^{13}\text{C}$  of bottom water within their calcite tests when they are alive and adding calcite, thus record a more instantaneous bottom water composition representative of only the time that the foraminifera was living on the sea floor (Curry et al., 1988). The lack of correlation of the foraminiferal records with the detrital fraction supports the notion that the shallow pore water  $\epsilon_{\text{Nd}}$  signal is a time-integrated deep water signal and is not modified by detrital inputs in this location. Furthermore the time period integrated across cannot be much longer than a few kyr or the glacial–interglacial shift would also have been lost, as would the unradiogenic values seen in the turbidite from BOFS 32K (Fig. S2).

#### 4.4. Glacial east–west deep water exchange in the low latitude Atlantic

The glacial  $\epsilon_{\text{Nd}}$  values we measured in the deep low latitude eastern Atlantic of around  $-10$  are similar to those observed in the abyssal northwest Atlantic (Bermuda Rise and Blake Ridge) during the LGM (Fig. 5; Gutjahr et al., 2008; Roberts et al., 2010). In contrast, the deep northern northeast Atlantic (Rockall Basin) and deep southeast Atlantic (Cape Basin) were both more radiogenic



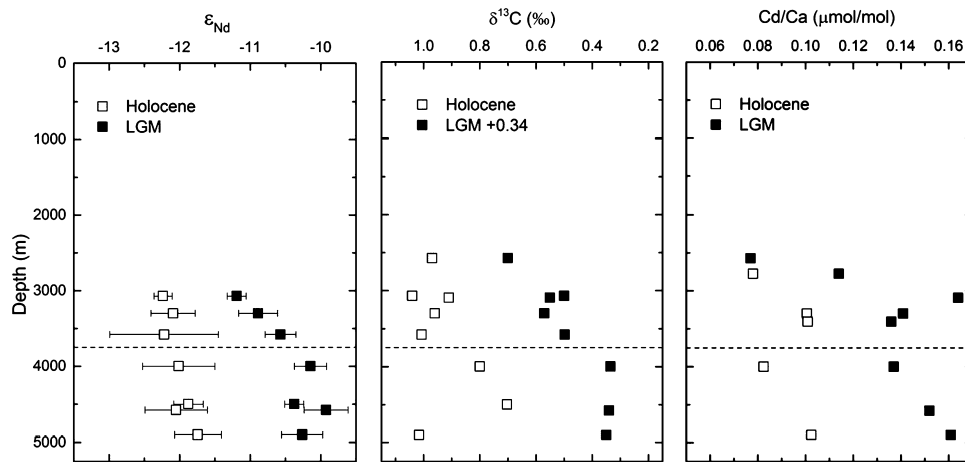


**Fig. 6.** Late Holocene (hollow squares) and Last Glacial Maximum (filled squares) (23–18 ka) reconstructions of the deep tropical eastern Atlantic from three paleoceanographic proxies. **Left:**  $\epsilon_{\text{Nd}}$  measured on uncleaned planktic foraminifera measured in this work on the cores listed in Table 1. **Middle:**  $\delta^{13}\text{C}$  of benthic foraminiferal calcite with  $+0.34\text{‰}$  added to glacial values to account for whole ocean shift (Peterson et al., 2014), note reversed x-axis to make glacial change in the same direction as the other proxies. **Right:** Cd/Ca ratio of benthic foraminifera. Core site locations and references for published  $\delta^{13}\text{C}$  and Cd/Ca data are given in Table S1. Dotted line on all three plots marks the sill depth of the Mid-Atlantic Ridge restricting communication between the eastern and western Atlantic at 3750 m (Metcalf et al., 1964).

with values around  $-6.5$  (Fig. 5). Our results reveal that the modified radiogenic seawater signal observed in the northern northeast Atlantic by Roberts and Piotrowski (2015) is not observed at the Mauritanian margin in the low latitude eastern Atlantic. Excluding those modified seawater values from the northern northeast Atlantic, the glacial  $\epsilon_{\text{Nd}}$  values throughout the Atlantic exhibit a gradient from least radiogenic in the north to most radiogenic in the south (Fig. 5), consistent with other studies (Howe et al., 2016; Lippold et al., 2016) and indicating the southwards export of glacial NADW. This conclusion is supported by the glacial benthic foraminiferal  $\delta^{13}\text{C}$  values from the same sites that are around  $+0.3\text{‰}$  in the northern northeast Atlantic,  $0.0\text{‰}$  in the tropical northeast Atlantic and as low as  $-1\text{‰}$  in the southeast Atlantic (Fig. 5). Even if the values in the southeast Atlantic include a Mackensen effect, the observation of the most positive values in the deep North Atlantic demonstrates that deep water was ageing in a north-to-south direction in the deep Atlantic during the LGM. The north to south ageing of deep waters in the Atlantic during the LGM can also be seen from radiocarbon ventilation ages that were lower in the deep North Atlantic than the deep South Atlantic (Skinner et al., 2014).

The difference in Nd isotopic composition between the foraminiferal  $\epsilon_{\text{Nd}}$  values of the five sites during the LGM (Figs. 3 and 6) is consistent with mixing between these northern- and southern-sourced deep waters with glacial  $\epsilon_{\text{Nd}}$  values around  $-13$  and  $-5.5$  respectively (Howe et al., 2016). In the glacial  $\epsilon_{\text{Nd}}$  profile (Fig. 6), a greater proportion of more radiogenic southern-sourced water is observed with increasing depth until the inflection point that occurs between the data points at 3600 and 4000 m, below which the composition is uniform with depth. This contrasts to the Holocene  $\epsilon_{\text{Nd}}$  profile for the region that is approximately uniform across the entire depth range of 3000 to 4900 m (Fig. 6) in agreement with modern salinity and  $\epsilon_{\text{Nd}}$  values in the eastern Atlantic (Fig. 2). The depth range of the glacial inflection point (3600 to 4000 m) encompasses the effective sill depth of the Mid-Atlantic Ridge at 3750 m (Metcalf et al., 1964). The same pattern of an increasing proportion of southern-sourced water with increasing depth down to  $\sim 3750$  m and a uniform deep water composition below  $\sim 3750$  m is evident in the glacial benthic foraminiferal  $\delta^{13}\text{C}$  profile for this region and could also be present in the glacial Cd/Ca profile although the latter data set is noisier than the former (Fig. 6).

We propose that the inflection point in these glacial profiles at  $\sim 3750$  m (dashed line, Fig. 6) represents the boundary between two water mass sources (1) abyssal water ventilating the eastern Atlantic via the Vema Fracture Zone below the sill depth of the Mid-Atlantic Ridge (3750 m) and (2) at depths shallower than 3750 m water masses flowing freely across from the western to the eastern Atlantic above the sill depth of the Mid-Atlantic Ridge. The water above 3750 m shows the same gradient of more southern-sourced water with increasing depth that has observed at similar latitudes in the glacial western Atlantic (Howe et al., 2016), thus the gradient is preserved during west-to-east advection. In contrast, we infer that the waters below 3750 m in the glacial eastern Atlantic were homogenised by their movement over rough bathymetry as they moved through equatorial fracture zones (Mercier and Morin, 1997; Metcalf et al., 1964) resulting a uniform mixture of northern- and southern-sourced water. Deep water reaching the low latitude eastern Atlantic directly from the north or the south during the LGM is ruled out as the Walvis Ridge prevents water coming from the south (Broecker et al., 1980) and, as discussed earlier, the deep northern northeast Atlantic showed much more radiogenic seawater  $\epsilon_{\text{Nd}}$  values during the LGM (Fig. 5) (Roberts and Piotrowski, 2015). This conclusion of ventilation from west to east during the LGM is supported by a glacial  $\epsilon_{\text{Nd}}$  value measured on a core from the deep western Atlantic near the latitude of the Vema Fracture Zone (Howe et al., 2016) that exhibits values very similar to those observed in the deep eastern Atlantic in this work (Fig. 7). Thus, our results imply that deep water entered the low latitude eastern Atlantic from the western Atlantic during the LGM via the same routes as compared to the modern ocean (Fig. 1) but that the water mass mixing proportions in the eastern Atlantic basin were different during glacial times. The abyssal eastern Atlantic was filled by a vertically homogeneous water mass, from 3750 m to the seafloor with an  $\epsilon_{\text{Nd}}$  of  $\sim -10$  and  $\delta^{13}\text{C}$  of  $\sim 0.0\text{‰}$ , due to the sub-sampling and mixing of two water masses from the western Atlantic. We conclude that the vertical homogeneity of waters below 3750 m in the glacial eastern Atlantic was not due to boundary exchange of slow moving waters as in that case we would have expected them to be shifted to less radiogenic values seen in benthic nepheloid layers in the modern ocean (Stichel et al., 2015), whereas instead they have a very similar composition of deep waters near the Vema Fracture Zone in the western Atlantic (Fig. 7). The ventilation regime inferred here that is analogous to the modern regime contrasts with the origi-



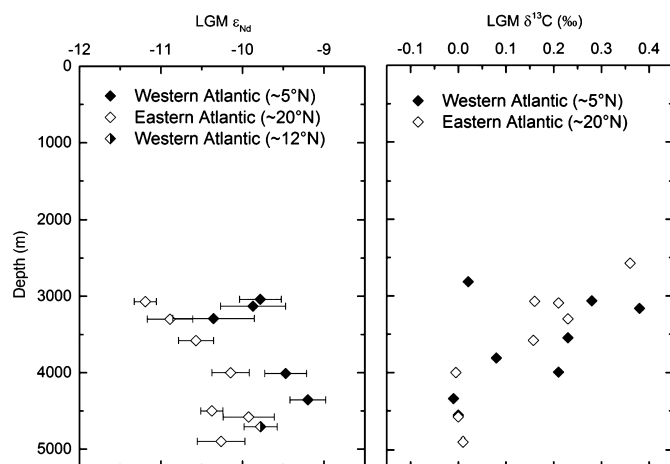


**Fig. 7.** Comparison of LGM (23–18 ka) authigenic  $\varepsilon_{\text{Nd}}$  (left) and benthic foraminiferal  $\delta^{13}\text{C}$  (right) depth transects for the Mauritanian margin at 20°N in the eastern Atlantic (hollow diamonds), and the Ceara Rise at 5°N in the western Atlantic (filled diamonds) as well as a single site from the Mid-Atlantic Ridge near the Vema Fracture Zone (half-filled diamond; V25-42). Neodymium results from the western Atlantic are from Howe et al. (2016) and Lippold et al. (2016). Carbon isotopes are from references in Table S2 for the eastern Atlantic and Curry and Lohmann (1990) and Howe et al. (2016) for the western Atlantic.

nal interpretation of the benthic foraminiferal  $\delta^{13}\text{C}$  and Cd/Ca data from these sites that AABW filled the abyssal western Atlantic during the LGM and flowed over the top of the Mid-Atlantic Ridge into the deep eastern Atlantic (Beveridge et al., 1995).

The net  $\varepsilon_{\text{Nd}}$  shift from the LGM to the late Holocene of these eastern Atlantic records being greater in the deeper sites (Fig. 6) is in agreement with a study that compiled the deglacial  $\varepsilon_{\text{Nd}}$  shifts from elsewhere in the deep Atlantic (Wei et al., 2016). Furthermore the shifts are similar to records from the Ceara Rise in the equatorial western Atlantic (Fig. 5) (Lippold et al., 2016). The net shifts at these low latitude sites of up to 2 epsilon units are, however, smaller than those seen elsewhere in the Atlantic (Fig. 5). This implies that the low latitude Atlantic saw a less significant change in water mass mixing proportions between glacial and interglacial conditions than many sites elsewhere in the Atlantic.

The Mauritanian margin sites, however, display less radiogenic glacial  $\varepsilon_{\text{Nd}}$  values than the Ceara Rise sites (Fig. 7). This observation implies that there was a greater proportion of northern-sourced deep water at 20°N in the eastern Atlantic than near the equator in the western Atlantic during the LGM. The eastern Atlantic  $\varepsilon_{\text{Nd}}$  values are, however, comparable with the inferred neodymium composition of waters at around 20°N in the glacial western Atlantic (Howe et al., 2016), consistent with the interpretation that waters were mixing across to our sites in the eastern Atlantic from the same latitudes in the western Atlantic during the LGM. Despite the different water mass mixing proportions inferred from  $\varepsilon_{\text{Nd}}$  profiles from the glacial western Atlantic near the equator and eastern Atlantic near 20°N the benthic foraminiferal  $\delta^{13}\text{C}$  values are very similar (Fig. 7). Given that glacial northern-sourced water had a higher  $\delta^{13}\text{C}$  than glacial southern-sourced water (Curry and Oppo, 2005) this observation implies that there must have been a greater amount of respired organic carbon in the glacial deep eastern Atlantic than the western Atlantic during the LGM lowering the  $\delta^{13}\text{C}$  values in the eastern Atlantic. This is analogous to situation in the modern ocean where nutrient concentrations are higher in the deep eastern Atlantic than the western Atlantic despite similar salinity values (Fig. 2) due to higher productivity and slower circulation in the eastern Atlantic (Broecker et al., 1980; Fariduddin and Loubere, 1997).

## 5. Conclusions

We present deglacial foraminiferal  $\varepsilon_{\text{Nd}}$  records from five cores, BOFS 28K–32K, on the Mauritanian margin in the deep low latitude eastern Atlantic Ocean and one core from the Ceara Rise in the deep equatorial western Atlantic. The low latitude eastern and western Atlantic exhibit very similar deglacial  $\varepsilon_{\text{Nd}}$  values at corresponding depths, with only slightly more radiogenic values at the more-southerly western Atlantic sites during the LGM. Contrasting the authigenic  $\varepsilon_{\text{Nd}}$  records from the eastern Atlantic with detrital  $\varepsilon_{\text{Nd}}$  values reveals that there is no evidence for the influence of Saharan dust on the down-core signal, either through boundary exchange via a benthic nepheloid layer or post-depositional diagenesis. More radiogenic  $\varepsilon_{\text{Nd}}$  values at all five sites during the LGM instead indicate a lesser influence of North Atlantic Deep Water in the deep low latitude eastern Atlantic at that time, consistent with other cores in the Atlantic. Our results show a neodymium isotope gradient during the LGM that we interpret as a mixture of northern- and southern-sourced waters from the western Atlantic ventilating the deep eastern Atlantic directly at depths above 3750 m and homogenised by west-to-east transport through the Vema Fracture Zone below 3750 m. This inference is supported by previously reported glacial  $\delta^{13}\text{C}$  and Cd/Ca profiles from the region. Collectively these observations reveal that during the LGM the deep low latitude eastern Atlantic was ventilated from the western Atlantic in the same manner as in the modern ocean. Comparison of the glacial depth profiles of eastern and western Atlantic  $\varepsilon_{\text{Nd}}$  and  $\delta^{13}\text{C}$  demonstrates that there was a greater amount of respired organic matter in the eastern Atlantic than in the western Atlantic during the LGM, which is analogous to modern Atlantic circulation.

## Acknowledgements

Samples were provided by the Godwin Laboratory for Paleoclimate Research at the University of Cambridge and the International Ocean Discovery Program. Data is listed in the supplementary material and available at [www.pangaea.de](http://www.pangaea.de). Radiocarbon analyses were supported by NERC radiocarbon grant 1752.1013 and Nd isotope analyses by NERC grants NERC NE/K005235/1 and NERC NE/F006047/1 to AMP. JNWH was supported by a Rutherford Memorial Scholarship. Natalie Roberts and Albert Galy are thanked for helpful discussions of these results and Simon Crowhurst, Steven Moreton, Jo Clegg, Jason Day and Sam Williams are thanked for technical support.

## Appendix A. Supplementary material

Supplementary material related to this article can be found online at <http://dx.doi.org/10.1016/j.epsl.2016.10.048>.

## References

- Barker, S., Kiefer, T., Elderfield, H., 2004. Temporal changes in North Atlantic circulation constrained by planktonic foraminiferal shell weights. *Paleoceanography* 19, PA3008. <http://dx.doi.org/10.1029/2004PA001004>.
- Beveridge, N.A.S., 1995. *Paleoceanography of the Eastern Atlantic*. University of Cambridge, Cambridge.
- Beveridge, N., Elderfield, H., Shackleton, N.J., 1995. Deep thermohaline circulation in the low-latitude Atlantic during the last glacial. *Paleoceanography* 10, 643–660.
- Böhm, E., Lippold, J., Gutjahr, M., Frank, M., Blaser, P., Antz, B., Fohlmeister, J., Frank, N., Andersen, M.B., Deininger, M., 2015. Strong and deep Atlantic meridional overturning circulation during the last glacial cycle. *Nature* 517, 73–76. <http://dx.doi.org/10.1038/nature14059>.
- Bory, A., 1997. Etude des flux de matériel terrigène dans la colonne d'eau de l'Atlantique subtropical nord-est: relations avec les apports atmosphériques. Doctoral thesis. Univ. Paris 7 Denis Diderot, p. 265.
- Boyle, E.A., Keigwin, L.D., 1987. North Atlantic thermohaline circulation during the past 20,000 years linked to high-latitude surface temperature. *Nature* 330, 35–40.

- Broecker, W.S., Takahashi, T., Stuiver, M., 1980. Hydrography of the central Atlantic-II waters beneath the two-degree discontinuity. *Deep-Sea Res.* 27A, 397–419. [http://dx.doi.org/10.1016/0198-0149\(80\)90052-7](http://dx.doi.org/10.1016/0198-0149(80)90052-7).
- Butzin, M., Prange, M., Lohmann, G., 2005. Radiocarbon simulations for the glacial ocean: the effects of wind stress, Southern Ocean sea ice and Heinrich events. *Earth Planet. Sci. Lett.* 235, 45–61. <http://dx.doi.org/10.1016/j.epsl.2005.03.003>.
- Charles, C., Fairbanks, R., 1992. Evidence from Southern Ocean sediments for the effect of North Atlantic deep-water flux on climate. *Nature* 355, 416–419.
- Cole, J.M., Goldstein, S.L., Peter, B., Hemming, S.R., Grousset, F.E., 2009. Contrasting compositions of Saharan dust in the eastern Atlantic Ocean during the last deglaciation and African Humid Period. *Earth Planet. Sci. Lett.* 278, 257–266. <http://dx.doi.org/10.1016/j.epsl.2008.12.011>.
- Curry, W.B., Duplessy, J., Labeyrie, L., Shackleton, N.J., 1988. Changes in the distribution of  $\delta^{13}\text{C}$  of deep water  $\text{CO}_2$  between the last glaciation and the Holocene. *Paleoceanography* 3, 317–341.
- Curry, W.B., Lohmann, G.P., 1983. Reduced advection into Atlantic Ocean deep eastern basins during last glaciation maximum. *Nature* 306, 577–580.
- Curry, W.B., Lohmann, G.P., 1990. Reconstructing past particle fluxes in the tropical Atlantic Ocean. *Paleoceanography* 5, 487–505.
- Curry, W.B., Oppo, D.W., 2005. Glacial water mass geometry and the distribution of  $\delta^{13}\text{C}$  of  $\Sigma\text{CO}_2$  in the western Atlantic Ocean. *Paleoceanography* 20, PA1017. <http://dx.doi.org/10.1029/2004PA001021>.
- Fariduddin, M., Loubere, P., 1997. The surface ocean productivity response of deeper water benthic foraminifera in the Atlantic Ocean. *Mar. Micropaleontol.* 32, 289–310. [http://dx.doi.org/10.1016/S0377-8398\(97\)00026-1](http://dx.doi.org/10.1016/S0377-8398(97)00026-1).
- Frank, M., 2002. Radiogenic isotopes: tracers of past ocean circulation and erosional input. *Rev. Geophys.* 40.
- Gherardi, J., Labeyrie, L., McManus, J., Francois, R., Skinner, L., Cortijo, E., 2005. Evidence from the Northeastern Atlantic basin for variability in the rate of the meridional overturning circulation through the last deglaciation. *Earth Planet. Sci. Lett.* 240, 710–723. <http://dx.doi.org/10.1016/j.epsl.2005.09.061>.
- Goldstein, S.L., Hemming, S.R., 2003. Long-lived isotopic tracers in paleoceanography and ice sheet dynamics. In: *Treatise on Geochemistry*. Elsevier Science Publishers B.V., pp. 453–489.
- Grousset, F.E., Parra, M., Bory, A., Martinez, P., Bertrand, P., Shimmield, G.B., Ellam, R.M., 1998. Saharan wind regimes traced by the Sr–Nd isotopic composition of subtropical Atlantic sediments: last Glacial Maximum vs today. *Quat. Sci. Rev.* 17, 395–409.
- Gutjahr, M., Frank, M., Stirling, C.H., Keigwin, L.D., Halliday, A.N., 2008. Tracing the Nd isotope evolution of North Atlantic Deep and Intermediate Waters in the western North Atlantic since the Last Glacial Maximum from Blake Ridge sediments. *Earth Planet. Sci. Lett.* 266, 61–77. <http://dx.doi.org/10.1016/j.epsl.2007.10.037>.
- Howe, J.N.W., Piotrowski, A.M., Noble, T.L., Mulitza, S., Chiessi, C.M., Bayon, G., 2016. North Atlantic Deep Water production during the Last Glacial Maximum. *Nat. Commun.* 7, 11765. <http://dx.doi.org/10.1038/ncomms11765>.
- Jacobsen, S.B., Wasserburg, G.J., 1980. Sm–Nd isotopic evolution of chondrites. *Earth Planet. Sci. Lett.* 50, 139–155.
- Jenkins, W.J., Smethie Jr., W.M., Boyle, E.A., Cutter, G.A., 2015. Water mass analysis for the U.S. GEOTRACES (GA03) north Atlantic Sections. *Deep-Sea Res., Part 2, Top. Stud. Oceanogr.* 116, 6–20. <http://dx.doi.org/10.1016/j.dsr2.2014.11.018>.
- Jullien, E., Grousset, F., Malaizé, B., Duprat, J., Sanchez-Goni, M.F., Eynaud, F., Charlier, K., Schneider, R., Bory, A., Bout, V., Flores, J.A., 2007. Low-latitude “dusty events” vs. high-latitude “icy Heinrich events”. *Quat. Res.* 68, 379–386. <http://dx.doi.org/10.1016/j.yqres.2007.07.007>.
- Lacan, F., Jeandel, C., 2005. Neodymium isotopes as a new tool for quantifying exchange fluxes at the continent–ocean interface. *Earth Planet. Sci. Lett.* 232, 245–257. <http://dx.doi.org/10.1016/j.epsl.2005.01.004>.
- Lacan, F., Tachikawa, K., Jeandel, C., 2012. Neodymium isotopic composition of the oceans: a compilation of seawater data. *Chem. Geol.* 300–301, 177–184. <http://dx.doi.org/10.1016/j.chemgeo.2012.01.019>.
- Lambelet, M., van de Fliedert, T., Crockett, K., Rehkämper, M., Kreissig, K., Coles, B., Rijkens, M.J.A., Gerringa, L.J.A., de Baar, H.J.W., Steinfeldt, R., 2016. Neodymium isotopic composition and concentration in the western North Atlantic Ocean: results from the GEOTRACES GA02 section. *Geochim. Cosmochim. Acta* 177, 1–29. <http://dx.doi.org/10.1016/j.gca.2015.12.019>.
- Lippold, J., Gutjahr, M., Blaser, P., Christner, E., Ferreira, M.L.D.C., Mulitza, S., Christl, M., Wombacher, F., Böhm, E., Antz, B., Cartapanis, O., Vogel, H., Jaccard, S.L., 2016. Deep water provenience and dynamics of the (de)glacial Atlantic meridional overturning circulation. *Earth Planet. Sci. Lett.* 445, 68–78. <http://dx.doi.org/10.1016/j.epsl.2016.04.013>.
- McCartney, M.S., Bennett, S.L., Woodgate-Jones, M.E., 1991. Eastward flow through the Mid-Atlantic Ridge at 11°N and its influence on the abyss of the eastern basin. *J. Phys. Oceanogr.* 21, 1089–1121.
- Mercier, H., Morin, P., 1997. Hydrography of the romanche and chain fracture zones. *J. Geophys. Res.* 102, 10373–10389. <http://dx.doi.org/10.1029/97JC00229>.
- Metcalfe, W.G., Heezen, B.C., Stalcup, M.C., 1964. The sill depth of the Mid-Atlantic Ridge in the equatorial region. *Deep-Sea Res. Oceanogr. Abstr.* 11, 1–10.
- Peterson, C.D., Lisiecki, L.E., Stern, J.V., 2014. Deglacial whole-ocean  $\delta^{13}\text{C}$  change estimated from 480 benthic foraminiferal records. *Paleoceanography* 29, 549–563. <http://dx.doi.org/10.1002/2013PA002552>.
- Piotrowski, A.M., Galy, A., Nicholl, J.A.L., Roberts, N., Wilson, D.J., Clegg, J.A., Yu, J., 2012. Reconstructing deglacial North and South Atlantic deep water sourcing using foraminiferal Nd isotopes. *Earth Planet. Sci. Lett.* 357–358, 289–297.
- Piotrowski, A.M., Goldstein, S.L., Hemming, S.R., Fairbanks, R.G., 2004. Intensification and variability of ocean thermohaline circulation through the last deglaciation. *Earth Planet. Sci. Lett.* 225, 205–220. <http://dx.doi.org/10.1016/j.epsl.2004.06.002>.
- Reimer, P., Bard, E., Bayliss, A., Beck, J.W., Blackwell, P.G., Ramsey, C.B., Buck, C.E., Cheng, H., Edwards, R.L., Friedrich, M., Grootes, P.M., Guilderson, T.P., Hafflidason, H., Hajdas, I., Hatté, C., Heaton, T.J., Hoffman, D.L., Hogg, A.G., Hughen, K.A., Kaise, K.F., Kromer, B., Manning, S.W., Niu, M., Reimer, R.W., Richard, D.A., Scott, E.M., Southon, J.R., Staff, R.A., Turney, C.S.M., van der Plicht, J., 2013. IntCal13 and Marine13 radiocarbon age calibration curves 0–50,000 years cal BP. *Radiocarbon* 55, 1869–1887. [http://dx.doi.org/10.2458/azu\\_js\\_rc.55.16947](http://dx.doi.org/10.2458/azu_js_rc.55.16947).
- Rhein, M., Stramma, L., Krahlmann, G., 1998. The spreading of Antarctic bottom water in the tropical Atlantic. *Deep-Sea Res., Part 1, Oceanogr. Res. Pap.* 45, 507–527. [http://dx.doi.org/10.1016/S0967-0637\(97\)00030-7](http://dx.doi.org/10.1016/S0967-0637(97)00030-7).
- Rickli, J., Frank, M., Halliday, A.N., 2009. The hafnium–neodymium isotopic composition of Atlantic seawater. *Earth Planet. Sci. Lett.* 280, 118–127. <http://dx.doi.org/10.1016/j.epsl.2009.01.026>.
- Roberts, N.L., Piotrowski, A.M., 2015. Radiogenic Nd isotope labeling of the northern NE Atlantic during MIS 2. *Earth Planet. Sci. Lett.* 423, 125–133. <http://dx.doi.org/10.1016/j.epsl.2015.05.011>.
- Roberts, N.L., Piotrowski, A.M., Elderfield, H., Eglinton, T.I., Lomas, M.W., 2012. Rare earth element association with foraminifera. *Geochim. Cosmochim. Acta* 94, 57–71. <http://dx.doi.org/10.1016/j.gca.2012.07.009>.
- Roberts, N.L., Piotrowski, A.M., McManus, J.F., Keigwin, L.D., 2010. Synchronous deglacial overturning and water mass source changes. *Science* 327, 75–78. <http://dx.doi.org/10.1126/science.1178068>.
- Sarnthein, M., Winn, K., Jung, S.J.A., Duplessy, J.C., Labeyrie, L., Erlenkeuser, H., Ganssen, G., 1994. Changes in east Atlantic deepwater circulation over the last 30,000 years: eight time slice reconstructions. *Paleoceanography* 9, 209–267.
- Shackleton, N.J., Hall, M.A., Vincent, E., 2000. Phase relationships between millennial-scale events 64,000–24,000 years ago. *Paleoceanography* 15, 565–569.
- Siddall, M., Khaliwala, S., van de Fliedert, T., Jones, K., Goldstein, S.L., Hemming, S.R., Anderson, R.F., 2008. Towards explaining the Nd paradox using reversible scavenging in an ocean general circulation model. *Earth Planet. Sci. Lett.* 274, 448–461. <http://dx.doi.org/10.1016/j.epsl.2008.07.044>.
- Skinner, L.C., Scrivner, A.E., Vance, D., Barker, S., Fallon, S., Waelbroeck, C., 2013. North Atlantic versus Southern Ocean contributions to a deglacial surge in deep ocean ventilation. *Geology* 41, 667–670. <http://dx.doi.org/10.1130/G34133.1>.
- Skinner, L.C., Waelbroeck, C., Scrivner, A.E., Fallon, S.J., 2014. Radiocarbon evidence for alternating northern and southern sources of ventilation of the deep Atlantic carbon pool during the last deglaciation. *Proc. Natl. Acad. Sci.* 111, 5480–5484. <http://dx.doi.org/10.1073/pnas.1400668111>.
- Stichel, T., Frank, M., Rickli, J., Haley, B.A., 2012. The hafnium and neodymium isotope composition of seawater in the Atlantic sector of the Southern Ocean. *Earth Planet. Sci. Lett.* 317–318, 282–294. <http://dx.doi.org/10.1016/j.epsl.2011.11.025>.
- Stichel, T., Hartman, A.E., Duggan, B., Goldstein, S.L., Scher, H., Pahnke, K., 2015. Separating biogeochemical cycling of neodymium from water mass mixing in the Eastern North Atlantic. *Earth Planet. Sci. Lett.* 412, 245–260. <http://dx.doi.org/10.1016/j.epsl.2014.12.008>.
- Tanaka, T., Togashi, S., Kamioka, H., Amakawa, H., Kagami, H., Hamamoto, T., Yuhara, M., Orihashi, Y., Yoneda, S., Shimizu, H., Kunimaru, T., Takahashi, K., Yanagi, T., Nakano, T., Fujimaki, H., Shinjo, R., Asahara, Y., Tanimizu, M., Dragusanu, C., 2000. JNdi-1: a neodymium isotopic reference in consistency with LaJolla neodymium. *Chem. Geol.* 168, 279–281. [http://dx.doi.org/10.1016/S0009-2541\(00\)00198-4](http://dx.doi.org/10.1016/S0009-2541(00)00198-4).
- Teal, L.R., Bulling, M.T., Parker, E.R., Solan, M., 2008. Global patterns of bioturbation intensity and mixed depth of marine soft sediments. *Aquat. Biol.* 2, 207–218. <http://dx.doi.org/10.3354/ab00052>.
- Tiedemann, R., Sarnthein, M., Shackleton, N.J., 1994. Astronomic timescale for the Pliocene Atlantic  $\delta^{18}\text{O}$  and dust flux of Ocean Drilling Program site 659. *Paleoceanography* 9, 619–638.
- Waelbroeck, C., Skinner, L.C., Labeyrie, L., Duplessy, J.-C., Michel, E., Vazquez Riveiros, N., Gherardi, J.-M., Dewilde, F., 2011. The timing of deglacial circulation changes in the Atlantic. *Paleoceanography* 26, PA3213. <http://dx.doi.org/10.1029/2010PA002007>.
- Wei, R., Abouchami, W., Zahn, R., Masque, P., 2016. Deep circulation changes in the South Atlantic since the Last Glacial Maximum from Nd isotope and multi-proxy records. *Earth Planet. Sci. Lett.* 434, 18–29. <http://dx.doi.org/10.1016/j.epsl.2015.11.001>.